Surface Science 603 (2009) 2556–2563

Contents lists available at ScienceDirect

Surface Science

journal homepage: www.elsevier.com/locate/susc

From bilayer to monolayer growth: Temperature effects in the growth of Ru on Pt(1 1 1)

A. Berkó [1], A. Bergbreiter, H.E. Hoster, R.J. Behm *

Institute of Surface Chemistry and Catalysis, Ulm University, D-89069 Ulm, Germany

ARTICLE INFO

Article history:
Received 2 January 2009
Accepted for publication 27 May 2009
Available online 12 June 2009

Keywords:
Metal epitaxy
Growth
Exchange
Scanning tunneling microscopy
Ru
Pt(1 1 1)

ABSTRACT

At temperatures around 373 K, Ru growth on Pt(1 1 1) proceeds via nucleation and growth of bilayer islands [H.E. Hoster et al., Phys. Chem. Chem. Phys. 3 (2001) 337]. The influence of the deposition temperature on the Ru growth behavior on Pt(1 1 1) was studied by scanning tunneling microscopy (STM) and Auger electron spectroscopy (AES) in the temperature range between 303 and 773 K. The data reveal a distinct change in the growth characteristics, most important the change from the growth of bilayer Ru islands to monolayer islands, at temperatures between 523 and 573 K. Based on AES data and on atomic resolution STM images, these changes are associated with the onset and increasing contribution of surface alloy formation via Pt–Ru exchange and, at $T > 673$ K, alloy formation in near surface regions. Consequences of these data for the mechanism of bilayer growth and the underlying physical origin are discussed.

1. Introduction

Nucleation and growth of ultra-thin metal films have attracted considerable interest in recent years, both because of the interest in the atomistic understanding of the growth process [1–3], and because of their use as model system for studying the functional properties of bimetallic materials, e.g., for catalytic or electro-catalytic applications [4–7] or for magnetic recording technology [8,9]. It was early noticed that in a number of metal-on-metal systems the growth behavior did not follow the usual pattern predicted by standard nucleation and growth theory [2], but varied distinctly in characteristic features. One example for that is Ru/Pt(1 1 1), which was shown to grow via bilayer islands, preferentially upon deposition at room temperature and almost exclusively at 373 K [10]. In addition, a distinct decoration of the Pt(1 1 1) steps by Ru islands was observed. A similar bilayer growth behavior was reported, but not yet understood on an atomistic scale, also for other systems such as Co/Cu(1 0 0) [11–13], Co/Cu(1 1 1) [14–17], Co/Pd(1 1 1) [18,19], Co/Au(1 1 1) [20,21], or Co/Ag(1 1 1) [21]. In these studies, it turned out that the growth characteristics depended strongly on the deposition temperature, with the bilayer growth changing to the expected growth via monolayer islands at higher temperatures. A more detailed understanding of the growth process and of the physical origin of the bilayer growth, which could be transferred to the present Ru/Pt(1 1 1) system, was, however, still lacking (see also Refs. [18,19,22,23] and for the present system Ref. [24]). Finally, growth of multilayer islands was observed also for Ru electrodeposition on Pt(1 1 1) electrodes [25–29].

Recently, we could show that the bilayer growth is a consequence of the stronger interaction between Ru and Ru compared to that of Pt–Ru, which favors Ru bilayer island growth compared to wetting of the Pt(1 1 1) surface; strain effects play a minor role in this case [24]. In the present paper, we report results of a combined Auger electron spectroscopy (AES) and scanning tunneling microscopy (STM) study on the growth of submonolayer Ru deposits on a Pt(1 1 1) surface, focusing on temperature effects in the growth behavior. This work is part of extensive studies in our laboratory on the correlation between structural and chemical properties of structurally well-defined bimetallic PtRu surfaces as model systems for state-of-the-art PtRu fuel cell anode catalysts [30,31], which include so far Pt monolayer modified Ru(0 0 0 1) surfaces [32–35] and monolayer $Pt_xRu_{(1-x)}$ surface alloys grown on a Ru(0 0 0 1) substrate [32,33,36–39]. Ru modification of Pt substrates, e.g., of Pt(1 1 1), is expected to result in surfaces with different electronic and structural properties. The preparation of monolayer Ru modified Pt(1 1 1) substrates would require a change in the bilayer growth characteristics. According to the previous results obtained on other bilayer growth systems [11–21], variation of the deposition temperature may be one way to reach this.

Following the presentation of our experimental data, we will compare these results with the findings for other metal-on-metal

* Corresponding author. Tel.: +49 731 50 25451; fax: +49 731 50 25452.
E-mail address: juergen.behm@uni-ulm.de (R.J. Behm).
[1] Address: Reaction Kinetics Research Laboratory, Institute of Nanochemistry and Catalysis, Chemical Research Center of the Hungarian Academy of Sciences, University of Szeged, H-6720 Szeged, Dóm tér 7, Hungary.

0039-6028/$ - see front matter © 2009 Elsevier B.V. All rights reserved.
doi:10.1016/j.susc.2009.05.033

systems with a similar bilayer growth process (see above, Refs. [11–21,23]), and discuss consequences and conclusions of these findings for the growth mechanism and the underlying physical origin.

2. Experimental

The measurements were performed in a standard ultrahigh vacuum (UHV) chamber (base pressure 6×10^{-9} Pa), which is equipped with a home-built pocket size STM and standard facilities for surface preparation and characterization. These include a cylindrical electron energy analyzer (Physical Electronics, CMA 10-155) for Auger electron spectroscopy, electron beam evaporators for Pt and Ru evaporation (Omicron EFM 3), a quadrupole mass spectrometer (Balzers, QMA 120) for residual gas analysis, and an Ar^+ ion gun for sample cleaning. Further details are given in Ref. [40].

The cleaning procedure consisted of cycles of Ar^+ bombardment (0.5 kV, 10 μA cm^{-2}, 15 min) and three subsequent annealing cycles up to 1100 K, followed by exposure to 1 Langmuir (1 L, 10 s $\times$ 10^{-7} mbar) O_2 during cool-down below 900 K, and two final annealing cycles up to 1050 K to remove carbon contaminations and adsorbed O. All annealing cycles were performed at controlled heating/cooling rates of 4 K s^{-1} (heating) and 2 K s^{-1} (cool-down), respectively. After this treatment, no contamination was detected by AES, and the clean Pt(1 1 1) surface was characterized by extended (50–100 nm), atomically smooth terraces. Atomic resolution images on the clean substrate or between the islands (see insets in Fig. 4c and d) did not show any impurities either, ruling out the presence of notable amounts of impurities such as carbon. Ru was evaporated at rates of around 0.2 monolayer (ML) min^{-1}. The deposition rate was tested regularly by STM measurements and found to be very stable. During evaporation, the background pressure was better than 6×10^{-8} Pa. STM images were collected in the constant current mode. The typical bias/current conditions for morphology and for atomic resolution imaging were 1.5 V/1 nA and 1 mV/100 nA, respectively. The surface morphology and the Ru coverage as well as the composition of the surface layer were determined by quantitative evaluation of the STM images.

3. Results and discussion

The effect of the substrate temperature on the growth behavior and hence on the morphology of the resulting Ru film was first explored by comparing the surface morphologies resulting upon deposition of 0.40 ± 0.04 ML of Ru at different temperatures (deposition rate 0.2 ML min^{-1}). This coverage was chosen for demonstration, since it illustrates the temperature effects most clearly. Fig. 1 shows a series of representative STM images (100 nm $\times$ 100 nm) recorded after Ru deposition on the clean Pt(1 1 1) surface at sample temperatures of (a) 303 K, (b) 373 K, (c) 473 K, (d) 523 K, (e) 573 K, (f) 623 K, (g) 673 K, and (h) 773 K.

The STM images provide detailed information on the characteristic trends and changes in the Ru growth behavior with increasing temperature, specifically on the evolution of the size, height, distribution, shape and density of the islands and on the surface area covered by them. Starting with the latter, they reveal that with increasing deposition temperature the fraction of the surface covered by adlayer islands first decreases, from around 34% for deposition at 303 K to ~22% at 373 K, then remains at constant values of 21–26% between 373 and 523 K, then increases drastically for 573 and 623 K to 32–41%, and finally starts to decrease at 673 K. For deposition at 773 K, the surfaces are essentially smooth, with very few island structures. The exact values of the island covered relative surface areas are listed in Table 1, together with other characteristic parameters. Parallel with these changes, the island heights change as well. The islands exhibit a clear preference for bilayer growth (island heights 0.41 ± 0.02 nm) at growth temperatures between 373 and 523 K, in agreement with previous findings for comparable deposition conditions (373 K) [10]. For deposition at lower temperatures (303 K), a tendency towards bilayer is visible as well, but not as pronounced as in the temperature regime between 373 and 523 K (mean island height 0.29 nm, see also Ref. [10]). For deposition above 523 K, monolayer islands prevail (island height around 0.23 ± 0.01 nm, see Table 1). (The absolute values of the island heights were determined by using the measured value (0.227 nm) of the Pt(1 1 1) step height as reference.) The Ru coverages calculated from the total volume of the adlayer islands vary only slightly, within ±10%, up to 623 K deposition temperature (see Table 1).

So far, the data indicate a clear change from bilayer growth at lower temperatures (at 303 K bilayer growth appears to be kinetically limited) to monolayer growth at higher temperatures, with a transition in the growth behavior in the temperature range between 523 and 573 K. There is, however, another important difference between the two temperature ranges. In the lower temperature range, the steps of the Pt(1 1 1) substrate are fully decorated by adlayer islands, while this is not the case for deposition temperatures of 573 K and above. At the higher temperatures, the step decoration by bilayer islands is replaced by a line of separate smaller monolayer islands on the upper terraces of the Pt(1 1 1) substrate, parallel to the steps.

The morphology of the islands on the terraces and along the steps is illustrated in the height profiles shown below the respective STM images in Fig. 1. The profiles represent the height variations along the lines indicated in the related images by black–white dotted lines. For better illustration of the island morphology, the height profiles are underlaid with a schematic representation of the local layer structure and composition of the islands and of the underlying substrate. These profiles not only demonstrate the distinct bilayer growth on the terraces, but also explain the decoration of Pt(1 1 1) substrate steps by Ru islands in a simple way. It results from the condensation of Ru adatoms at the ascending steps of the Pt(1 1 1) substrate, leading to Ru island nucleation ('heterogeneous nucleation') along the step edge. The stabilization of bilayer island configurations results in a continuous line of bilayer islands (referenced to the lower terrace surface) along the ascending steps. Attachment of Ru adatoms coming from the upper terrace allows these islands to grow also on the upper terrace, where they form monolayer islands, which then can stabilize an additional Ru layer on top. The line of monolayer islands formed at higher deposition temperatures parallel to the steps on the upper terraces, at a distance of about 4 nm from the steps, can be explained by heterogeneous nucleation along a boundary between two different substrate materials. This boundary is created by Ru attachment at the ascending steps (Pt–Ru transition) or by surface alloy formation along the steps, e.g., by embedding of Ru adatoms in a stripe along the steps. For deposition at 673 K, one can clearly see that island nucleation is inhibited on the lower terrace in a strip of 4 nm width along the ascending step, which can be explained by the reduced density of Ru adatoms in this area due to Ru attachment/incorporation at the ascending steps.

In Fig. 2a, the relative amounts of island material in the first three adlayers at ~0.4 ML are plotted as a function of the deposition temperature. The plot clearly demonstrates that the material in the higher layers and thus the fraction of bilayer islands drops suddenly in the temperature range of 523–573 K, and monolayer islands become the typical configuration.

The island density first decreases from 303 K (Fig. 1a, 1.27×10^{12} cm^{-2}) to 373 K (Fig. 1b, 0.56×10^{12} cm^{-2}) deposition temperature. Upon increasing the deposition temperatures

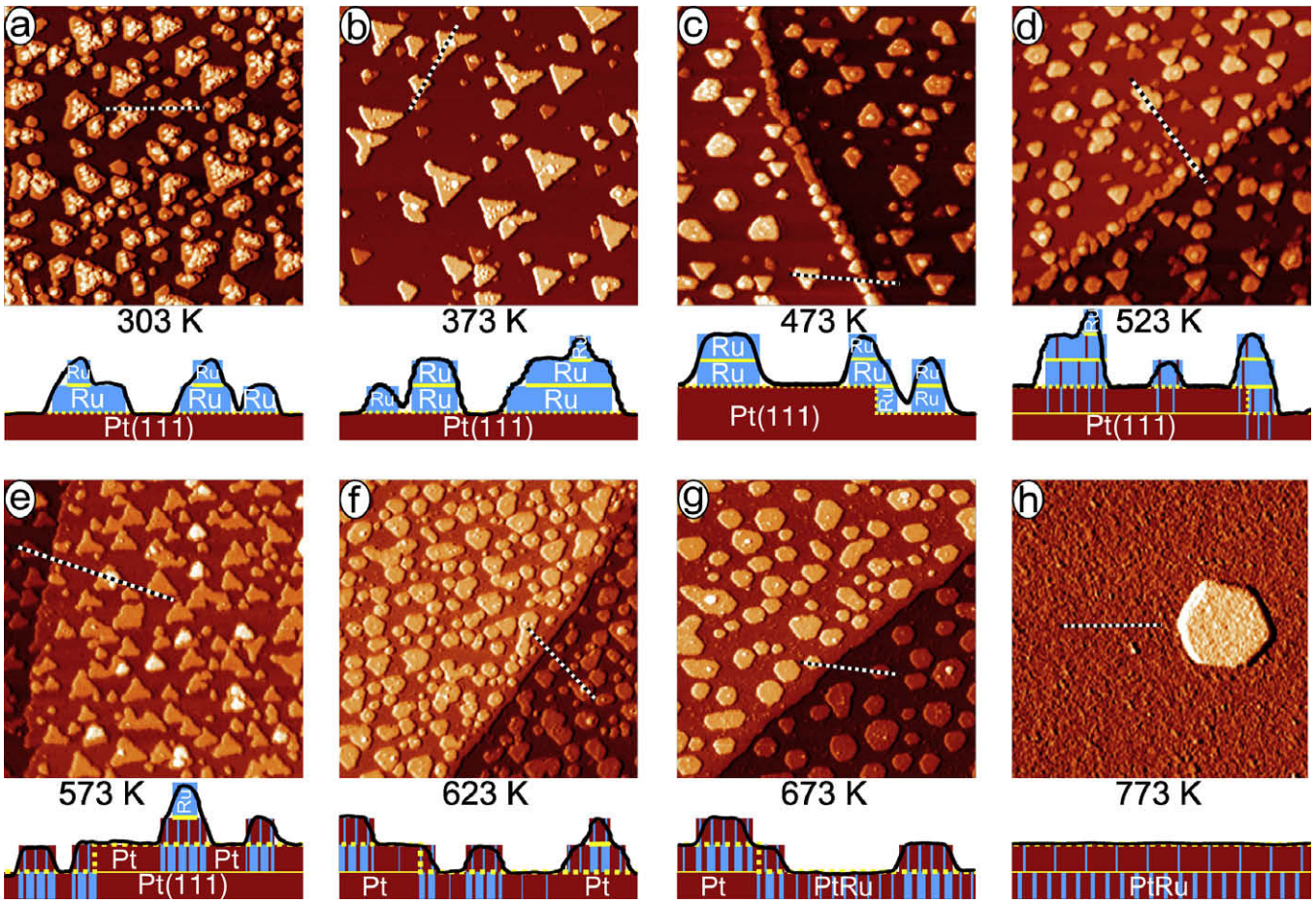

Fig. 1. Representative STM images ($100 \times 100\ nm^2$) recorded after deposition of (a) 303 K; (b) 373 K; (c) 473 K; (d) 523 K; (e) 573 K; (f) 623 K; (g) 673 K; and (h) 773 K. The deposition rate was 0.20 ML min^{-1} in each case. Below the STM images, height profiles of the respective surface are shown, which show a cut along the black–white dotted lines in the respective STM images. The morphology of the islands and of the underlying substrate along the cut is indicated schematically in these profiles, furthermore, the chemical composition of the island and the substrate surface layer, as derived from the data in Figs. 2–4, is illustrated. Striped patterns indicate (surface) alloy formation and the alloy composition in the respective layer.

Table 1
Characteristic features of the islands formed by deposition of 0.40 (±0.04) ML Ru on Pt(1 1 1) at different deposition temperatures (deposition rate 0.2 ML/min). The possible error in all values is approximately ±10%, for the height measurements the height of the monoatomic Pt(1 1 1) steps of 0.227 nm was used as a reference. Mean island height are calculated via the height distribution of the islands.

Growth characteristics	Growth temperature						
	303 K	373 K	473 K	523 K	573 K	623 K	673 K
Fraction of the surface covered by the islands in percent	34 ± 2	22 ± 2	25 ± 1	26 ± 1	32 ± 3	38 ± 4	29 ± 2
Mean island height (nm)	0.29 ± 0.01	0.40 ± 0.03	0.40 ± 0.04	0.39 ± 0.04	0.25 ± 0.03	0.22 ± 0.01	0.22 ± 0.01
Ru coverage calculated from the total volume of the islands (ML)	0.41 ± 0.02	0.39 ± 0.03	0.42 ± 0.03	0.44 ± 0.03	0.35 ± 0.03	0.38 ± 0.04	0.29 ± 0.02
Island density (10^{12} cm^{-2})	1.27 ± 0.13	0.56 ± 0.02	0.82 ± 0.10	1.14 ± 0.11	1.38 ± 0.14	2.14 ± 0.21	1.19 ± 0.12
Typical island shape	Roughly triangular	Triangular	Triangular	Hexagonal/ triangular	Triangular	Hexagonal	Hexagonal
Decoration of the Pt(1 1 1) steps by Ru bilayer islands (yes/no)	Yes	Yes	Yes	Yes	No	No	No

(473–623 K), however, this trend turns around and the island density increases again slightly: 0.82×10^{12} cm^{-2} (473 K), 1.14×10^{12} cm^{-2} (523 K), 1.38×10^{12} cm^{-2} (573 K) and 2.14×10^{12} cm^{-2} (623 K) (average error ± 10%), respectively (Fig. 1c–f). This increase is in contrast to expectations based on standard nucleation theory, where increasing temperature results in a decreasing density of stable nuclei [2]. Possible reasons for this discrepancy will be discussed below. Together with the growing island density and the constant island volume, the average island size, which is in the range of 7–10 nm, decreases slightly up to 523 K, until at 573 K the island size increases due to the transition to monolayer islands. At higher deposition temperatures (673 K), the nucleation behavior returns again to the normal trends, and the saturation island density decreases with temperature to 1.2×10^{12} cm^{-2} at 673 K (Fig. 1g) and almost complete absence of islands on the 500–100 nm wide terraces at 773 K deposition temperature. The decrease in island density is accompanied by a significant increase in island size (10–12 nm at 673 K).

Finally, also the shape of the adlayer islands undergoes characteristic changes with increasing deposition temperature. For deposition at 303 and 373 K, small compact islands with no regular shapes and larger triangular islands are formed. The sides of the

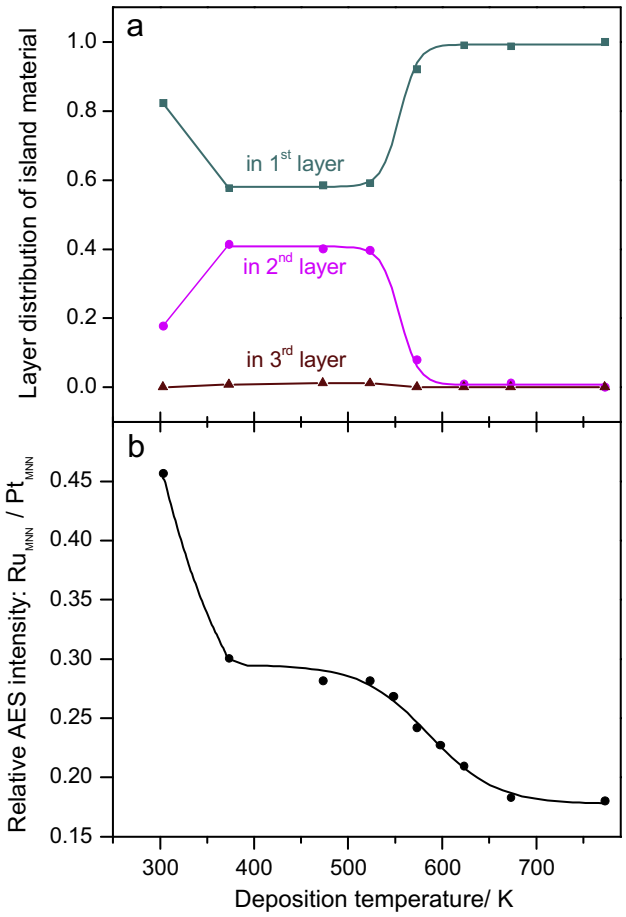

Fig. 2. (a) Distribution of the island material on the different layers after deposition of similar amounts of Ru (0.40 ± 0.04 ML) at increasing deposition temperatures (303–773 K, temperatures see figures). (b) Relative Ru intensity R_{Ru} ($R_{Ru} = I_{Ru\ 273\ eV}/I_{Pt\ 64\ eV}$) measured after deposition of similar amounts of Ru (0.40 ± 0.04 ML) as a function of the deposition temperature.

triangular islands are oriented along the close packed directions of the Pt(1 1 1) terraces. As expected for an fcc(1 1 1) surface, the island orientation does not vary between subsequent terraces. Uniformly oriented triangular islands are a common phenomenon in metal-on-metal growth [3]. The absence of a preferential island shape for the small islands can be explained by kinetic effects. For the small island sizes the mobility of the adatoms along the island edges and corners is still too high to develop distinct triangular island shapes [41,42]. For deposition at 473–523 K, part of the islands develops more compact, relaxed hexagonal shapes. Nevertheless, for the temperature range dominated by bilayer growth, triangular island shapes are characteristic (Fig. 1a–d). This is true even for deposition at 573 K, where monolayer growth sets in (Fig. 1e). Deviations from a simple triangular shape, which are more frequent at lower deposition temperatures, are attributed to two different effects, (i) limited mobility of adatoms along the island edges and corners, and (ii) coalescence of adjacent nuclei during deposition. At higher deposition temperatures (623 and 673 K), the monolayer islands exhibit distorted hexagonal shapes. The changes in island shape and island growth kinetics are attributed to increasing rates of vertical exchange processes between Ru and Pt atoms, which change the composition of the islands and the underlying substrate layer. This will be discussed in more detail below.

In addition to STM imaging, we performed complementary AES measurements after Ru deposition at similar conditions as used for the STM measurements. In each case, approximately 0.40 ML of Ru was deposited. The AES spectra were measured immediately after Ru deposition. The ratios between the peak-to-peak intensities of the Ru_{MNN} peak (273 eV) and the Pt_{MNN} signal (64 eV), the relative Ru Auger intensities R_{Ru}, are plotted as function of the deposition temperature in Fig. 2b. The relative Auger intensity R_{Ru} has its maximum value of 0.45 at 303 K and drops to 0.3 at 373 K. This decrease results from the transition to enhanced bilayer growth at 373 K, where less Ru is in the outermost layer. In the temperature range of 373–523 K, it decreases only slightly from 0.30 to 0.27. A significant decay, however, occurs between 523 and 673 K, where it drops to 0.19. This decay of R_{Ru} coincides with the dramatic change in the morphology and/or composition of the deposited Ru layer in the temperature range of 523–573 K. A simple transition from bilayer to monolayer growth of Ru at 523–573 K would lead to a re-increase of the R_{Ru} value at higher temperatures, which is opposite to the trend observed in the experiments. This apparent contradiction can be resolved if we assume that in this temperature range Ru atoms in the growing islands start to exchange with Pt surface atoms and this way form a surface alloy with increasing Pt contents in the adlayer islands and Ru contents in the substrate surface layer underneath the islands. (Incorporation of the Ru atoms in the surface layer of the Pt(1 1 1) substrate alone would not affect the value of R_{Ru}.) This process does not modify the amount of material in the islands, in agreement with the experimental observation of a constant island volume up to 623 K. Only if the exchanged surface atoms and the Ru adatoms become sufficiently mobile on the surface that the mean distance between the islands approaches the average terrace width, the measured island volume will start to decay. Furthermore, since at these rather low temperatures extensive solution of Ru in the bulk can be excluded (self diffusion of Pt in Pt bulk sets in at above 1400 K [43]), the Ru content in the near surface regions should be maintained. The much more facile Ru → Pt surface exchange compared to Ru bulk dissolution can be rationalized by the lower coordination of the surface atoms. The less stringent geometric confinement of the neighboring atoms at the surface reduces the barrier for exchange, while for bulk dissolution and hence for bulk diffusion the neighboring atoms are essentially fixed to their position. Based on our experiments, bulk dissolution is possible only for temperatures at around 773 K and above. Thermodynamically, the exchange of Ru deposit atoms and Pt surface atoms is driven by the highly positive segregation energy of Ru in Pt, which favors bulk dissolution of Ru in Pt rather than surface segregation of Ru. This agrees perfectly with results from density functional calculations, which equally yielded high positive values for the segregation energy of Ru in Pt [23,44,45]. Comparing Ru accumulation in the near surface regions of the Pt substrate, e.g., in the subsurface layer, and homogeneous dissolution of Ru in the Pt bulk, the latter is favored entropically. This contribution is significant at the temperatures required from kinetic reasons (sufficient mobility of the Ru atoms). Furthermore, additional contributions may arise from a stabilization of Ru in the subsurface layer, underneath Pt surface atoms. Though a precise, quantitative determination of the extent of subsurface exchange and bulk diffusion is not possible from the present AES data, they clearly indicate that the onset of Ru bulk diffusion is at least 300–400 K higher compared to Ru surface exchange.

The variation of the island density with deposition temperature, which is plotted in Fig. 3 (see also Table 1), differs significantly from the behavior expected from standard nucleation and growth theory [2]. According to the latter theory, we would expect a continuous decay of the saturation island density n_s with increasing deposition temperature. While between 303 and 373 K the island density decreases as expected, we find a clear increase of the island density in the temperature range of 373–623 K. The unusual

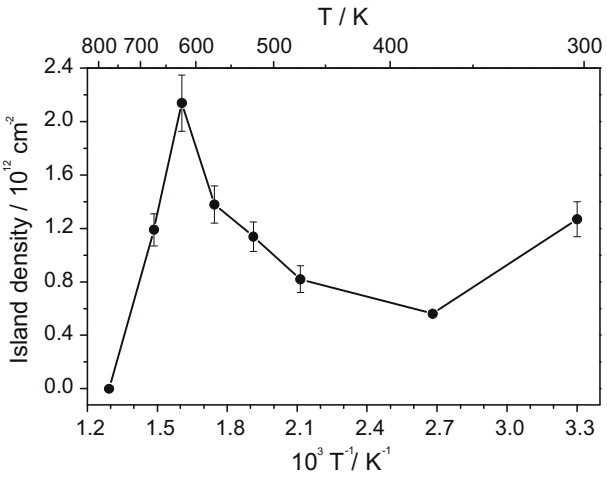

Fig. 3. Variation of the island density with the (inverse) deposition temperature for deposition of ~0.40 ML Ru on Pt(1 1 1).

behavior of the island density overlaps with the transition from bilayer to monolayer growth (523 → 573 K) and with the onset of Ru exchange with Pt surface atoms (⩾523 K), as evidenced by the AES data in Fig. 2b. Similar deviations from the predicted nucleation behavior were reported earlier already for a few other metal-on-metal growth systems such as Ni/Ag(1 1 1) [46] and Co/Cu(0 0 1) [47], where the island density was found to first decrease and then increase with temperature, before it finally decreased again. The increasing island density above a critical temperature was explained by a combination of two effects, an increasing tendency for thermally activated exchange of Ni (Co) adatoms with Ag(1 1 1) (Cu(1 0 0)) surface atoms with temperature, and a stabilization of Ni (Co) adatoms and small adlayer islands by underlying Ni (Co) atoms in the substrate surface layer [46–48]. Hence, the exchanged Ni (Co) atoms act as nucleation sites for the heterogeneous nucleation and growth of Ni (Co) adlayer islands. A similar mechanism was predicted also for Rh growth on Ag(1 0 0) [49,50] and for the systems Ni/Ag(1 0 0) [51], Fe/Au(1 0 0) [52], Au/Ni(1 1 0) [53], and Fe/Cu(1 0 0) [54–56]. At temperatures above 523 K, the stabilization of adlayer nuclei by incorporated Ru atoms decreases and the system reverts to the 'normal' nucleation and growth behavior. Thus, the distinct deviation of the temperature dependent variation in Ru island density from trends predicted by standard nucleation and growth theory is in full agreement with our above conclusions that at temperatures >523 K exchange of Ru adatoms and Pt(1 1 1) surface atoms plays an important role for Ru growth on Pt(1 1 1). Furthermore, they indicate that Ru–Pt surface exchange starts already at much lower temperatures, between 373 and 473 K.

The most direct and convincing evidence for intermixing and surface alloy formation in the Ru islands, however, comes from atomic resolution STM images with chemical contrast [32,57–59]. Although on the island covered surfaces atomically resolved imaging was rather difficult to achieve due to the steep increase at the island edges, especially for the bilayer islands, atomic resolution images of the islands with chemical contrast could be obtained. (The difficulties in atomic resolution imaging result from the close distance between tip and surface required for atomic resolution imaging, which in particular at island edges lead to considerable forces between tip and surface, which can in turn induce material displacement at these positions.) Examples obtained on differently grown surfaces are shown in Fig. 4. Fig. 4a shows the surface morphology of a 2.1 ML Ru film deposited at 473 K, i.e., close to the temperature where the dominant islands change from bilayer to monolayer height. As expected, ~55% of each terrace is covered by bilayer islands (the numbers in Fig. 4a indicate the local thickness in ML). According to the atomically resolved image in Fig. 4b, the second layer consists of at least two species that differ in their apparent brightness. We clearly find a number of 'dark' surface atoms on the image (~2–3% of the total number of surface atoms), and a few brighter surface atoms in a matrix of similar height surface atoms. The two surface components Pt and Ru are identified by comparison with atomic resolution images of different PtRu/Ru(0 0 0 1) surface alloys, where Pt surface atoms corresponded to 'dark' atoms, i.e., Pt surface atoms led to a local decrease of the tunnel current [38]. A similar electronic effect is expected also for the present situation, despite of the different substrate and the slightly different lattice constant, and the dark sites in the island are associated with Pt surface atoms. This assignment of Ru being the majority species is supported by the AES data (see Fig. 2), which at this temperature only show a small decrease of R_{Ru} compared to the lower temperatures. The rather complex contrast situation in the STM images, with more than two contrast levels, is probably caused by local variations in the composition of the subsurface layer. The situation resembles that on bulk alloy surfaces, where similar observations were reported and interpreted in the same way [60–62]. Variations in the apparent heights and thus in the local electronic properties due the presence of impurities such as carbon are considered as unlikely (see Section 2), and are therefore ruled out as origin of the additional height levels.

A second set of data was recorded on a surface covered with bilayer islands upon Ru deposition at 523 K (0.3–0.4 ML Ru, Fig. 4c). Based on similar assumptions as described above, the surface layer in these islands contains about 10–15% Pt. Hence, the bilayer islands do not consist purely of Ru, but contain non-negligible amounts of Pt, at least, if they are deposited at temperatures close to the transition from bilayer to monolayer island growth. The inset in Fig. 4c shows the terrace area between the islands with atomic resolution. This and other images show essentially no indication for incorporated Ru atoms in the surface layer between the adlayer islands, which supports our previous conclusion that Ru atoms are mainly located within the bilayer islands (see above discussion to Fig. 2b).

The situation is very different for the monolayer islands. Fig. 4d shows an image recorded on top of a single monolayer island, on a monolayer island covered surface grown at 573 K deposition temperature. In that image, the bright Ru atoms are no more dominant, but are embedded in an adlayer island, which predominantly consists of Pt atoms. Based on a quantitative evaluation of the image, approximately 80–90% of the surface atoms in the adlayer island are Pt atoms. Atomic resolution imaging of the terrace areas in between the islands (see inset in Fig. 4d) indicates that also at 573 K incorporation of Ru atoms in the exposed Pt(1 1 1) substrate is very unlikely. Accordingly, most of the Ru deposited on the surface should be immersed in the Pt surface layer underneath the monolayer islands, due to exchange of the Pt and Ru atoms during deposition. This interpretation, which is illustrated in the schematic model of the surface in Fig. 1e, is supported also by the distinct decrease of the relative Ru Auger intensity R_{Ru} observed upon deposition at 573 K (Fig. 2b).

The last images in this series (Fig. 4e and f) finally show an island covered area of a surface after deposition of 0.8 ML Ru at 673 K. Because of the higher Ru coverage, the second layer population is higher than that listed in Table 1 (0.4 ML). Although individual atoms are not resolved in the enlarged view in Fig. 4f, the short scale variation in apparent height clearly indicates a bimetallic composition of the surface layer in the adlayer, similar to observations for deposition at 573 K. Furthermore, we find a similar structure also in the areas between the terraces, i.e., for deposition at 673 K both adlayer islands and terrace areas consist of a Pt-rich, mixed surface layer of about similar composition, presumably with

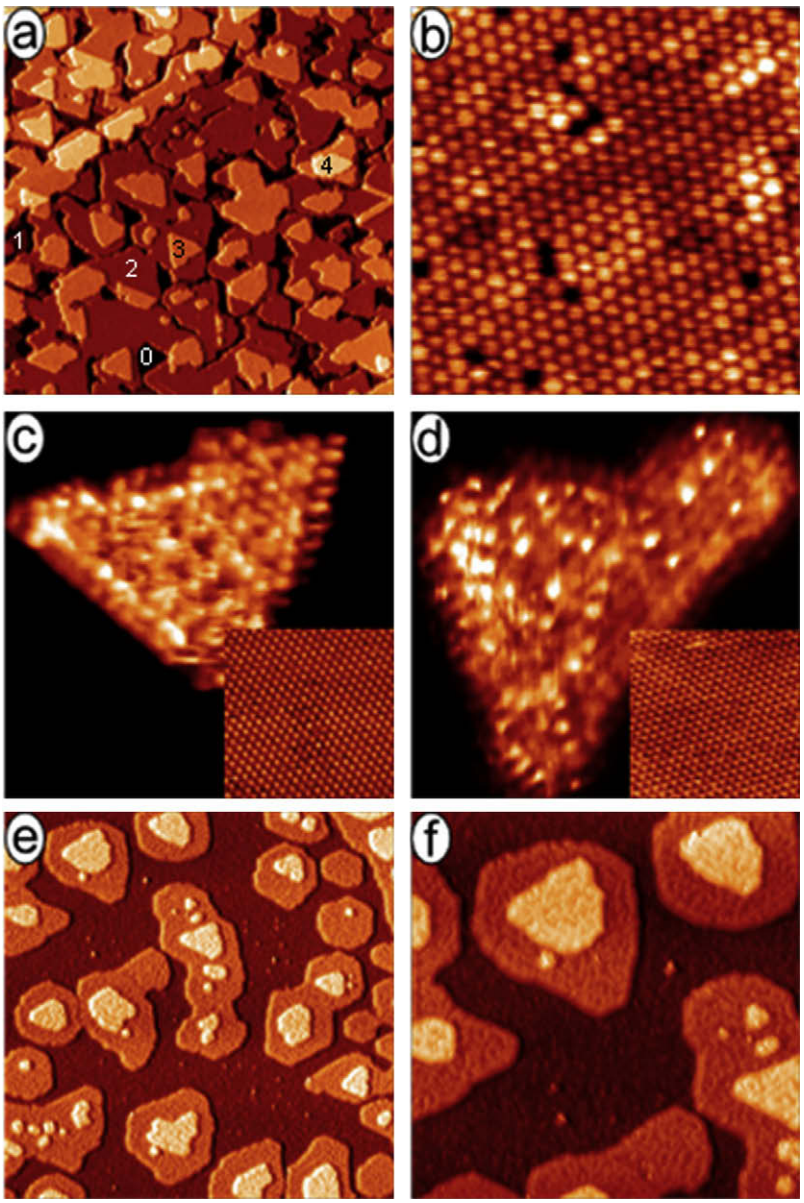

Fig. 4. STM images showing the mesoscopic ((4a, e): $100 \times 100\ nm^2$; (4f) $50 \times 50\ nm^2$) and atomic scale ((4b)–(4d), $5 \times 5\ nm^2$) structure after deposition of different amounts of Ru at different temperatures: (a) 2.1 ML Ru deposited at 473 K; numbers indicate local film thickness in ML; (b) atomic scale details of the 3rd island level with chemical contrast; (c): 0.4 ML Ru deposited at 523 K (surface composition on a bilayer island), inset: atomically resolved area of the exposed Pt terrace; (d): 0.4 ML Ru deposited at 573 K (surface composition on a monolayer island, inset: atomically resolved area of the exposed Pt terrace); (e), (f) monolayer island and terrace area on a surface after deposition of 0.8 ML Ru at 673 K; the corrugation indicates a homogeneous surface alloy formation in the different exposed layers.

a Ru-rich layer underneath. The presence of Ru in near surface regions is evident from the AES data in Fig. 2b.

Overall, the atomic resolution STM images confirm our previous conclusion that Ru adatoms start to exchange with Pt surface atoms already at temperatures significantly below the transition to monolayer growth or the onset of the decaying relative Ru intensity in AES measurements (~523 K both). At 473 K, individual incorporated Pt atoms are clearly resolved in Ru bilayer islands, and for 523 K deposition, the Pt surface content reaches 10–15%. Therefore it is likely that Ru exchange starts at temperatures between 373 and 473 K, in excellent agreement with our above conclusions derived from the Ru island densities. Monolayer islands grown by deposition at $\geqslant$573 K mainly consist of Pt (80–90% for deposition at 573 K), and Ru atoms are assumed to be in the subsurface layer underneath the island. Based on the close correlation between Pt surface content in the monolayer islands and the transition from bilayer to monolayer island growth, we propose that the stabilization of bilayer islands is linked to a critical Pt content in the monolayer islands. At higher Pt surface contents, the stabilization of the second island layer becomes too weak to support preferential bilayer growth, and normal layer growth with predominantly monolayer islands prevails. At lower Pt contents in the monolayer islands, and hence higher Ru contents, bilayer island growth dominates, driven by a stronger binding of Ru to Ru than to Pt. It should be pointed out that the second island layer contains more metal atoms than have landed on top of the growing monolayer islands during the deposition process. Hence, also transport of Ru and Pt adatoms from the large terraces onto the islands must be kinetically feasible even at room temperature.

Since the STM images show no indication of mixed surface layers in the areas between the islands for deposition at 573 K and below, exchange and surface alloy formation occur mostly at the adlayer islands during growth in the submonolayer coverage range. We suggest that exchange proceeds mostly during island

growth at the perimeter of the growing island. Here exchange is energetically more facile because of the less stringent geometric conditions than within the Ru islands. In addition to the exchange at the island perimeter, however, the incorporation of individual mobile Ru atoms in the Pt surface layer, which can act as nucleation sites for adlayer islands, becomes increasingly probable. This results in the increase of the island density with temperature.

Finally it should be noted that the varying composition of the islands and of the subsurface layer underneath the islands are likely to affect also the island shape, both the kinetically stabilized forms and the thermodynamic island shape. The relaxed hexagonal island shapes observed for deposition at 623 and 673 K are interpreted as the thermodynamically stable form of monolayer islands consisting of a Pt-rich adlayer and a Ru-rich surface substrate layer underneath. The bilayer growth mode makes the stable shape of monolayer Ru islands on a non-modified Pt(1 1 1) substrate experimentally not accessible. For the Ru-rich bilayer islands, we observe a transition from a mixture of irregular and relaxed triangular (Fig. 1a and b) to a mixture of relaxed triangular and hexagonal (Fig. 1c and d) island shapes for increasing growth temperatures, in the range from 303 → 523 K. This suggests a thermodynamic preference of the relaxed hexagonally shaped islands. Also in this case, final proof must come from theory, since experimentally the higher temperatures required to clearly overcome kinetic barriers are not accessible without changing the island composition.

For the Ru-rich bilayer islands (on an largely unmodified Pt(1 1 1) substrate) we assume that the small amounts of incorporated Pt atoms will not affect the stable island shape. Nevertheless, since because of their different compositions we can not directly compare monolayer and bilayer islands, the conclusion of relaxed hexagonal equilibrium shape of the bilayer islands is plausible, but not fully conclusive. Also in this case, final proof must come from theory, since experimentally the higher temperatures required to clearly overcome kinetic barriers are not accessible without changing the island composition.

In total, the study revealed a close correlation between the exchange of Ru adatoms or adlayer atoms and Pt substrate surface atoms and the general growth behavior. Ru atoms start to exchange into the Pt surface layer at temperatures between 373 and 573 K and act as nuclei for nucleation and growth of adlayer islands. Because of the thermal activation of the exchange process, this results in an increasing island density with temperature, up to 623 K. Exchange further controls the layer growth behavior, with growth of almost pure Ru bilayer islands up to 523 K, and monolayer island growth with predominantly Pt in the adlayer and exchanged Ru in the former substrate surface layer underneath at higher temperatures (>523 K). Both configurations are thermodynamically stable if bulk dissolution of Ru is inhibited but exchange between Ru adatoms and Pt surface atoms is possible (monolayer Pt islands), or if both Ru bulk dissolution and surface exchange of Ru are essentially inhibited (Ru bilayer islands). In a strict sense, both configurations are metastable with respect to bulk dissolution. The transition from mono- to bilayer growth is proposed to occur at a critical Pt content in the monolayer island surface layer.

4. Conclusions

Studying the temperature dependence of the growth of Ru on Pt(1 1 1) in the range between 303 and 773 K by STM and AES, we arrived at the following conclusions on the mechanism for Ru growth:

1. At temperatures below 523 K, Ru grows in pseudomorphic bilayer islands with a largely triangular shape (larger islands) or compact shape (small islands). The bilayer growth is explained by the strong Ru–Ru interactions, which leave bilayer islands energetically favorable compared to wetting the Pt(1 1 1) surface by monolayer islands. Exchange between Ru adatoms and Pt surface atoms and hence surface alloy formation are improbable, but not completely ruled out for temperature higher than 373 K: Ru atoms incorporated into the Pt surface layer, which stabilize Ru adlayer nuclei and this way act as nucleation sites for Ru adlayer islands, lead to an increasing island density with increasing deposition temperatures for deposition at >373 K, in contrast to the trend expected from standard nucleation and growth theory.
   Ru adatoms condensing at ascending Pt(1 1 1) steps act as nuclei for bilayer Ru islands at steps and to step decoration by Ru bilayer islands (relative to the lower terrace), lateral Ru growth onto the upper terrace cause bilayer island growth along the steps also on this terrace.
2. At temperatures around 523 K, exchange between Ru adatoms and Pt surface atoms becomes significant during (sub-)monolayer film growth. Bilayer island growth still prevails, but atomic resolution STM images with chemical contrast resolve intermixing in the surface layer of the bilayer islands, with about 10–15% Pt in the surface layer. Exchange mainly occurs at the growing islands, the amount of Ru surface atoms incorporated in the Pt(1 1 1) surface in areas between the islands is negligible.
3. At temperatures between 523 and 573 K, the stabilization of bilayer islands becomes weaker and bilayer island growth changes into monolayer island growth. The transition is associated with a critical Pt content in the monolayer islands, at lower Pt (=higher Ru) contents in the first island layer bilayer islands are more stable, while for higher Pt contents, resulting from more efficient Ru → Pt(1 1 1) surface exchange, monolayer islands with predominantly Pt in the adlayer and exchanged Ru atoms in the topmost substrate layer prevail.
   Due to the decay of bilayer island stabilization, nucleation of bilayer islands at steps and hence the decoration of Pt steps with Ru bilayer islands ceases. Ru adatoms attaching at ascending steps are likely to intermix with Pt in the upper terrace layer.
4. At temperatures above the transition from monolayer to bilayer growth, in the range between 573 and 623 K, the tendency for Ru → Pt exchange increases further with increasing deposition temperature, and monolayer islands with predominantly Pt in the adlayer and exchanged Ru atoms in the topmost substrate layer dominate. This goes along with a change from triangular to relaxed hexagonal island shapes.
5. At temperatures around and above 673 K, the decreasing coverage of islands and mixed monolayer strips condensed at former Pt(1 1 1) steps points to the onset of step flow growth, where the increasing adatom mobility leads to the attachment of Ru and exchanged Pt adatoms at the ascending Pt(1 1 1) steps. Exchange of Ru adatoms and Pt surface atoms is facile also in the areas between the islands, and results in comparable Pt-rich surface composition and Ru-rich subsurface compositions in terrace areas and monolayer islands. For Ru deposition at 773 K, the island coverage is essentially zero and smooth surfaces prevail, which is attributed to a dominant step flow monolayer growth under these conditions, in combination with surface alloy formation. Ru bulk dissolution, which is thermodynamically favored, starts at or above 773 K.

Acknowledgements

This work was supported by the Landesstiftung Baden-Württemberg, within the Network Functional Nanostructures. One of the authors (A. Berkó) gratefully acknowledges financial support

by the Alexander von Humboldt Foundation and the Hungarian Scientific Research Fund (project OTKA – K69200).

References

[1] E. Bauer, in: D.A. King, D.P. Woodruff (Eds.), The Chemical Physics of Solid Surfaces and Heterogeneous Catalysis, vol. 3, Elsevier, Amsterdam, 1983.
[2] J.A. Venables, Surf. Sci. 299/300 (1994) 798.
[3] H. Brune, Surf. Sci. Rep. 31 (1998) 121.
[4] C.T. Campbell, Annu. Rev. Phys. Chem. 41 (1990) 775.
[5] J.A. Rodriguez, Surf. Sci. Rep. 24 (1996) 223.
[6] J.H. Sinfelt, Surf. Sci. 500 (2002) 923.
[7] J.G. Chen, C.A. Menning, M.B. Zellner, Surf. Sci. Rep. 63 (2008) 201.
[8] J. Shen, J. Kirschner, Surf. Sci. 500 (2002) 300.
[9] S.D. Bader, Surf. Sci. 500 (2002) 172.
[10] H.E. Hoster, T. Iwasita, H. Baumgärtner, W. Vielstich, Phys. Chem. Chem. Phys. 3 (2001) 337.
[11] H. Li, B.P. Tonner, Surf. Sci. 237 (1990) 141.
[12] A.K. Schmid, J. Kirschner, Ultramicroscopy 42–44 (1992) 483.
[13] J.R. Cerda, P.L. De Andres, A. Cebollada, R. Miranda, E. Navas, P. Schuster, C.M. Schneider, J. Kirschner, J. Phys. C: Condens. Mat. 5 (1993) 2055.
[14] V. Scheuch, K. Potthast, B. Voigtländer, H.P. Bonzel, Surf. Sci. 318 (1994) 115.
[15] J. de la Figuera, J.E. Prieto, C. Ocal, R. Miranda, Surf. Sci. 307 (1994) 538.
[16] S. Speller, S. Degroote, J. Dekoster, G. Langouche, J.E. Ortega, A. Närmann, Surf. Sci. 405 (1998) L542.
[17] J.E. Prieto, J. de la Figuera, R. Miranda, Phys. Rev. B 62 (2000) 2126.
[18] M. Wasniowska, N. Janke-Gilman, W. Wulfhekel, M. Przybylski, J. Kirschner, Surf. Sci. 601 (2007) 3073.
[19] M. Wasniowska, W. Wulfhekel, M. Przybylski, J. Kirschner, Phys. Rev. B 78 (2008) 035405.
[20] B. Voigtländer, G. Meyer, N.M. Amer, Phys. Rev. B 44 (1991) 10354.
[21] K. Morgenstern, J. Kibsgaard, J.V. Lauritsen, E. Laesgaard, F. Besenbacher, Surf. Sci. 601 (2007) 1967.
[22] B. Voigtländer, G. Meyer, N.M. Amer, Surf. Sci. 255 (1991) L529.
[23] A.V. Ruban, H.L. Skriver, J.K. Nørskov, in: D.P. Woodruff (Ed.), Surface Alloys and Alloy Surfaces, vol. 10, Elsevier, Amsterdam, 2002.
[24] A. Bergbreiter, A. Berkó, P.M. Erne, H.E. Hoster, R.J. Behm, Vacuum, doi:10.1016/j.vacuum.2009.04.001, in press.
[25] K.A. Friedrich, K.-P. Geyzers, A. Marmann, U. Stimming, R. Vogel, Z. Phys. Chem. 208 (1998) 137.
[26] E. Herrero, J.M. Feliu, A. Wieckowski, Langmuir 15 (1999) 4944.
[27] T. Iwasita, H. Hoster, A. John-Anacker, W.-F. Lin, W. Vielstich, Langmuir 16 (2000) 522.
[28] A. Crown, I.R. Moraes, A. Wieckowski, J. Electroanal. Chem. 500 (2001) 333.
[29] A. Crown, C. Johnston, A. Wieckowski, Surf. Sci. 506 (2002) L268.
[30] B.A. Peppley, J.C. Amphlett, R.F. Mann, in: W. Vielstich, A. Lamm, H.A. Gasteiger (Eds.), Handbook of Fuel Cells – Fundamentals Technology and Applications, Vol. 3: Fuel Cells and Technology, vol. 3, Wiley, Chichester, 2003.
[31] A. Hamnett, in: W. Vielstich, H.A. Gasteiger, A. Lamm (Eds.), Electrocatalysis, vol. 2, Wiley and Sons, Chichester, 2003.
[32] F. Buatier de Mongeot, M. Scherer, B. Gleich, E. Kopatzki, R.J. Behm, Surf. Sci. 411 (1998) 249.
[33] T. Diemant, T. Hager, H.E. Hoster, H. Rauscher, R.J. Behm, Surf. Sci. 541 (2003) 137.
[34] H.E. Hoster, B. Richter, R.J. Behm, J. Phys. Chem. B 108 (2004) 14780.
[35] T. Diemant, T. Hager, H. Rauscher, R.J. Behm, in preparation.
[36] H. Rauscher, T. Hager, T. Diemant, H. Hoster, F. Buatier de Mongeot, R.J. Behm, Surf. Sci. 601 (2007) 4608.
[37] T. Diemant, H. Rauscher, R.J. Behm, J. Phys. Chem. C 112 (2008) 8381.
[38] H.E. Hoster, A. Bergbreiter, P. Erne, T. Hager, H. Rauscher, R.J. Behm, Phys. Chem. Chem. Phys. 10 (2008) 3812.
[39] H.E. Hoster, R.J. Behm, in: M.T.M. Koper (Ed.), Fuel Cell Catalysis: A Surface Science Approach, Wiley and Sons, Chichester, 2008 (Chapter 14).
[40] E. Kopatzki, R.J. Behm, Surf. Sci. 245 (1991) 255.
[41] H. Brune, C. Romainczyk, H. Röder, K. Kern, Nature 369 (1994) 469.
[42] H. Brune, H. Röder, K. Bromann, K. Kern, J. Jacobsen, P. Stoltze, K. Jacobsen, J.K. Nørskov, Surf. Sci. 349 (1996) L115.
[43] M. Ondrejcek, W. Swiech, G. Yang, C.P. Flynn, Phil. Mag. Lett. 84 (2004) 69.
[44] A. Christensen, A.V. Ruban, P. Stoltze, K.W. Jacobsen, H.L. Skriver, J.K. Nørskov, F. Besenbacher, Phys. Rev. B 56 (1997) 5822.
[45] A.V. Ruban, H.L. Skriver, J.K. Nørskov, Phys. Rev. B 59 (1999) 15990.
[46] J.A. Meyer, R.J. Behm, Surf. Sci. 322 (1995) L275.
[47] R. Pentcheva, K. Fichthorn, M. Scheffler, T. Bernhard, R. Pfandzelter, H. Winter, Phys. Rev. Lett. 90 (2003) 076101.
[48] F. Nouvertné, U. May, M. Bamming, A. Rampe, U. Korte, G. Güntherodt, R. Pentcheva, M. Scheffler, Phys. Rev. B 60 (1999) 14382.
[49] S.-L. Chang, J.-M. Wen, P.A. Thiel, S. Günther, J.A. Meyer, R.J. Behm, Phys. Rev. B 53 (1996) 13747.
[50] L.D. Roelofs, D.A. Chipkin, C.J. Rockwell, R.J. Behm, Surf. Sci. 524 (2003) L89.
[51] R. Dorsch, Diploma Thesis, Ulm University, 1999.
[52] Y.-L. He, G.-C. Wang, Phys. Rev. Lett. 71 (1993) 3834.
[53] L.P. Nielsen, F. Besenbacher, I. Stensgaard, E. Laegsgaard, C. Engdahl, P. Stoltze, K.W. Jacobsen, J.K. Nørskov, Phys. Rev. Lett. 71 (1995) 754.
[54] K.E. Johnson, D.D. Chambliss, R.J. Wilson, S. Chiang, J. Vac. Sci. Technol. A 11 (1993) 1654.
[55] K.E. Johnson, D.D. Chambliss, R.J. Wilson, S. Chiang, Surf. Sci. 313 (1994) L811.
[56] D.D. Chambliss, K.E. Johnson, Phys. Rev. B 50 (1994) 5012.
[57] M. Schmid, H. Stadler, P. Varga, Phys. Rev. Lett. 70 (1993) 1441.
[58] R. Wiesendanger, M. Bode, R. Pascal, W. Allers, U.D. Schwarz, J. Vac. Sci. Technol. A 14 (1996) 1161.
[59] W.A. Hofer, G. Ritz, W. Hebenstreit, M. Schmid, P. Varga, J. Redinger, R. Podloucky, Surf. Sci. 405 (1998) L514.
[60] P. Weigand, P. Novacek, G. van Husen, T. Neidhart, P. Varga, Surf. Sci. 269–270 (1992) 1129.
[61] A. Biedermann, M. Schmid, P. Varga, Phys. Rev. B 50 (1994) 17518.
[62] P.T. Wouda, B.E. Nieuwenhuys, M. Schmid, P. Varga, Surf. Sci. 359 (1996) 17.